Measurement and Simulation of Memory Effects in Predistortion Linearizers

WOLFGANG BÖSCH AND GIULIANO GATTI, MEMBER, IEEE

Abstract —**A typical method for designing a predistortion linearizer is to realize a circuit that creates an AM/AM and AM/PM characteristic inverse to that of the power amplifier to be linearized [1]–[3]. This strategy is correct only if the predistortion circuit maintains this characteristic also at signal envelope frequencies. This is often not true due to the time constants present in the linearizer circuits that limit its effectiveness (hereafter these effects are referred as memory effects). This problem is not limited to linearization techniques but affects the operation of nonlinear systems in general. The purpose of this paper is to review the major consequences of memory effects, to present efficient techniques to measure them, and to illustrate a simulation approach that can be used to predict their influence in practical systems.**

I. Theoretical Background

IN GENERAL a nonlinear memoryless system may only cause an amplitude, never a phase, distortion. If a phase distortion is present, the system must possess a certain amount of memory [4]. Nonlinear systems with a small memory (in the sense that the circuit time constants are much smaller than the reciprocal value of the maximum envelope frequency) can be considered as quasi-memoryless systems. In this case at a certain instant the amount of amplitude and phase distortion depends only on the input signal level at the same time instant. Therefore most of the quasi-memoryless systems can be modeled only by their P_{in}/P_{out} characteristics (AM/AM conversion) and their amplitude-dependent phase shift characteristic (AM/PM conversion) [5].

For systems with larger memory, however, the AM/AM and AM/PM characteristics do not contain complete information about the nonlinearity, so the accuracy of this model is reduced. A precise characterization and simulation require more complex describing techniques, for example, the use of Volterra series representation [6] (see Fig. 1).

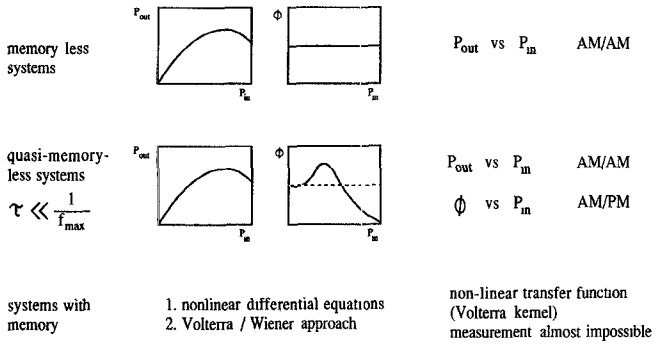

Fig. 1. Description of nonlinear systems.

II. Experimental Results on a Linearized *L*-Band Power Amplifier

The following example illustrates clearly the effects of memory in a 20 W power amplifier utilizing bipolar devices and linearized by means of a predistorting network. Figs. 2 and 3 show the characteristics of the nonlinearized and the linearized amplifier. Even though the AM/AM and AM/PM characteristics of the linearized amplifier appear much more linear (the gain compression of the linearized amplifier has been reduced by 3 dB), the two-carrier intermodulation test does not show any improvement compared to the nonlinearized power amplifier (Fig. 4).

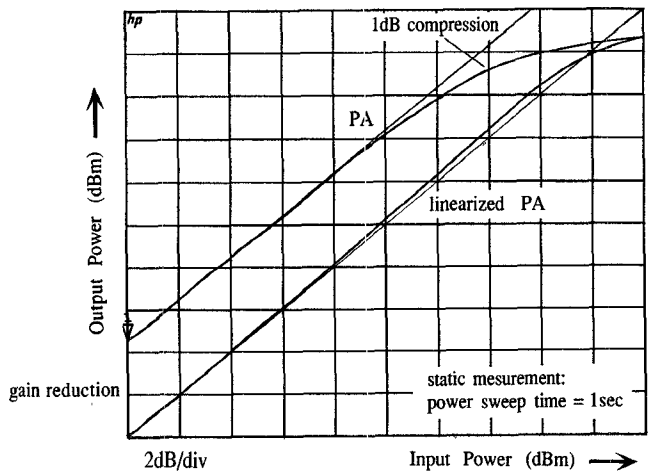

Fig. 2. Experimental results: AM/AM characteristic of a nonlinearized and a linearized amplifier.

This is a typical consequence of the presence of a nonnegligible memory in this system. In fact, even though the amplifier is statically linearized, its characteristics change with envelope frequencies. Therefore, if memory is present, the dynamic behavior of a linearized amplifier could be far from linear.

Manuscript received April 3, 1989; revised July 10, 1989.

The authors are with the RF Systems Division, European Space Agency Research and Technology Centre, NL-2200 AG Noordwijk, The Netherlands.

IEEE Log Number 8930815.

0018-9480/89/1200-1885$01.00 ©1989 IEEE

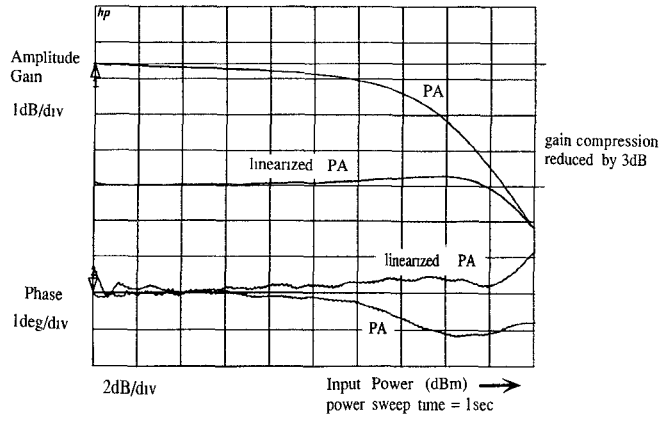

Fig. 3. AM/AM and AM/PM characteristics of a nonlinearized and a linearized amplifier.

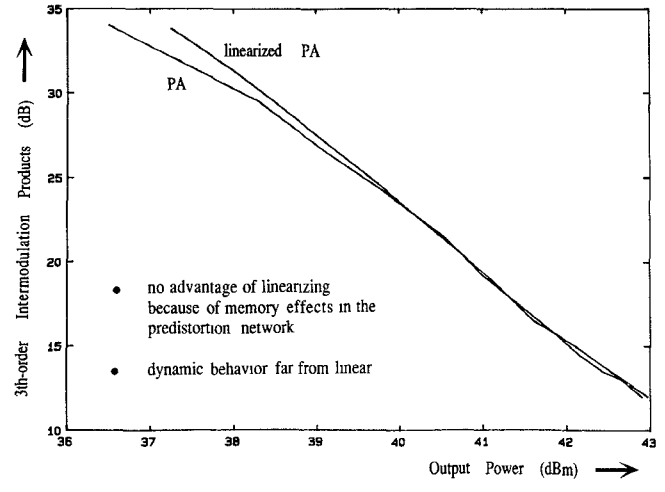

Fig. 4. Intermodulation measurement of the nonlinearized and the statically linearized amplifier with memory.

III. New Dynamic AM/AM and AM/PM Measurement Technique

A single-carrier power sweep measurement is very helpful during the design of power amplifiers. It also aids in adjusting linearizing circuits, but as the previous example illustrates, it does not provide any information about the system's memory and therefore significant differences may result between predicted and measured performance. On the other hand, performing a two-carrier measurement, which provides the memory information, does not directly give information about the AM/AM and AM/PM characteristics of the system; therefore it is not very useful in optimizing a linearizer characteristic on the bench.

Fig. 5 shows a schematic of a new dynamic power sweep measurement which combines both advantages [7]. The input signal is a two-carrier signal, which is swept over power. During the power sweep both carriers are synchronized; hence their amplitude is equal all the time. By means of two network analyzers (NWA's) the amplitude distortion and phase distortion of both of these carriers are measured.

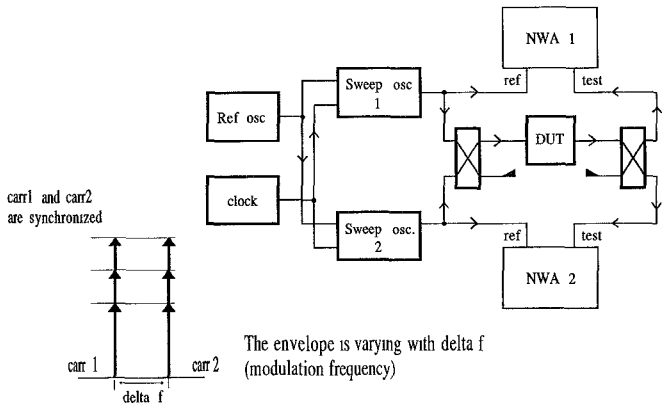

Fig. 5. Dynamic AM/AM and AM/PM measurement setup (dynamic power sweep).

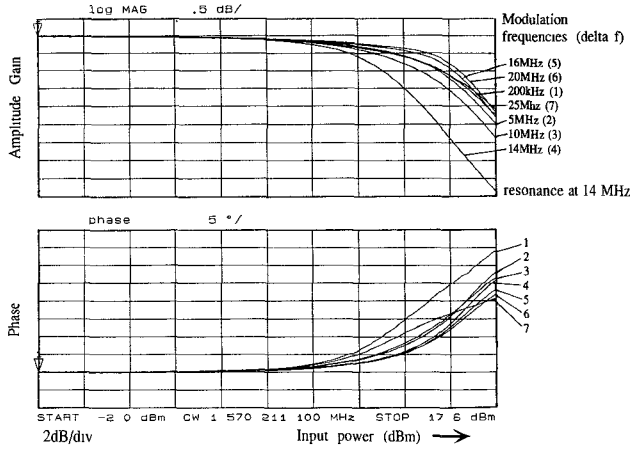

Fig. 6. Dynamic AM/AM and AM/PM measurement of an amplifier with memory effects.

Compared to a traditional power sweep measurement performed with one carrier, the envelope of the input signal varies with the two-carrier frequency separation ("delta f" in Fig. 5) and the AM/AM and AM/PM characteristics are measured dynamically (1):

$$A * [\cos(\omega_1 * t) + \cos(\omega_2 * t)] = 2A * \cos[(\omega_1 - \omega_2)/2 * t] * \cos[(\omega_1 + \omega_2)/2 * t]$$

where the modulation frequency, ω_m, is given by

$$\omega_m = \omega_1 - \omega_2. \quad (1)$$

Fig. 6 illustrates an amplifier with a nonnegligible memory. Clearly there is a "resonance frequency," where the compression and the phase characteristics are strongly dependent on the modulation frequency.

By changing the values of some blocking capacitors and inductors in the biasing circuit, the memory effects of this amplifier have been reduced. Fig. 7 shows the characteristic of the improved amplifier, which is clearly demonstrated by this technique to be quasi-memoryless and thus well behaved at all modulation frequencies. Such an amplifier can be successfully described by a traditional AM/AM and AM/PM measurement.

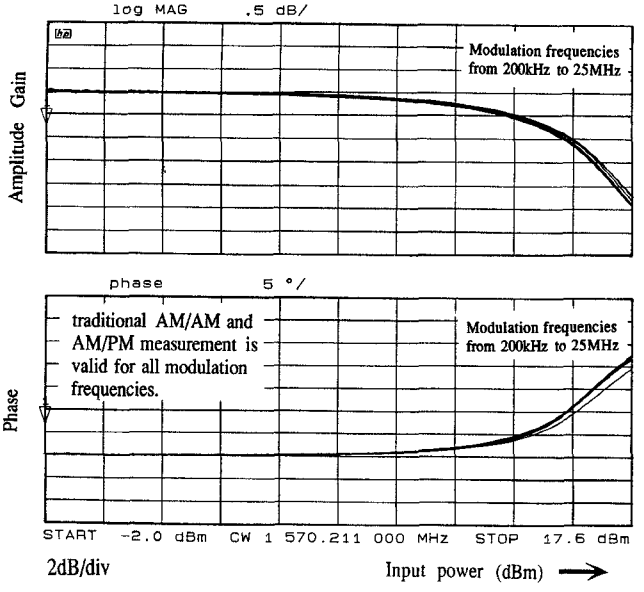

Fig. 7. Dynamic AM/AM and AM/PM measurement of a quasi-memoryless amplifier.

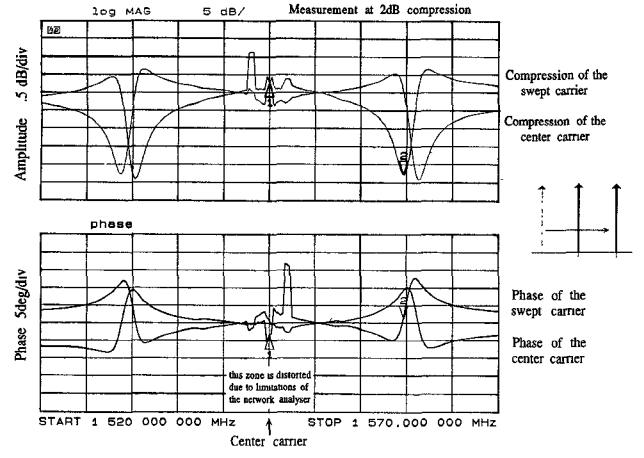

Fig. 8. Dynamic measurement in the frequency domain of an amplifier with memory.

Utilizing the same measurement setup but operating the amplifier at constant input power, we can also monitor with a NWA the amplitude and the phase of one carrier while sweeping the other carrier over frequency. In this way the changes in compression and phase are measured as a function of different envelope frequencies at a certain signal power level.

Fig. 8 gives a typical example of an amplifier with memory. The fixed carrier is located in the center of the plot. The traces show the change in compression (phase) of both the fixed and the swept carrier over envelope modulation frequency. Clearly, a resonance effect can be seen at a modulation frequency of about 14 MHz.

On the other hand, Fig. 9 illustrates the measurement results of an improved amplifier, where the memory effects have been removed.

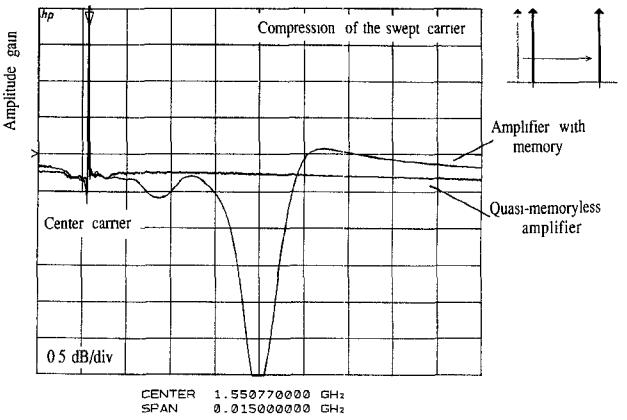

Fig. 9. Comparison of an amplifier with and without memory effects (dynamic measurement in the frequency domain).

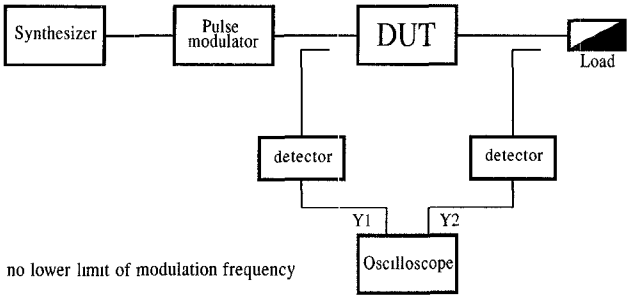

Fig. 10. Pulse power measurement setup.

By monitoring the memory effects in real time, the predistorter and the amplifier (especially their biasing networks) can easily be tuned to reduce the memory effects.

IV. Pulse Power Measurement System

This alternative system has the advantage of allowing the detection of very long time constant memories such as those caused by thermal effects or long time constants in biasing circuits, which are not clearly shown by the system previously described. In fact, the measurement setup shown in the previous section has a lower limit in the modulation frequency determined by the IF of the NWA.

Fig. 10 shows the basic measurement setup. The input signal is pulse modulated and drives the nonlinear system under test. The degraded output signal is detected by a wide-band power detector and visualized on an oscilloscope. In order to avoid overlapping of different pulse distorting effects, the pulse rise time has to be well selected between the lower limit, the smallest time constant of the memory to be detected, and the upper limit, the reciprocal value of the RF bandwidth of the amplifier and the detector system. A value of 0.5 μs has been used in the tests performed.

Measurement curves are reported in Fig. 11, where a significant long time constant memory is shown. Some kind of overshooting is visible, where in the first moment the amplifier delivers more output power than after several microseconds. In this particular case the amplifier operates

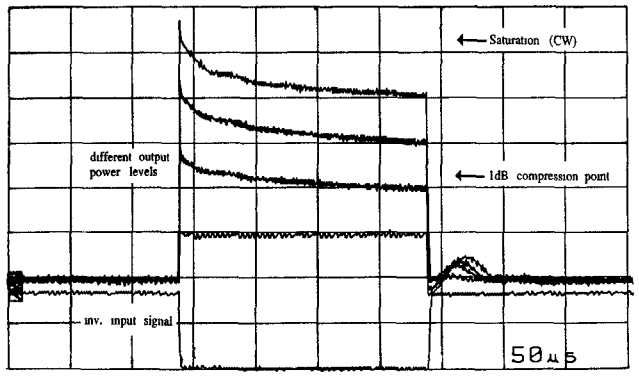

Fig. 11. Pulse power measurement of an amplifier with memory (overshooting effects due to long-time-constant memory effects).

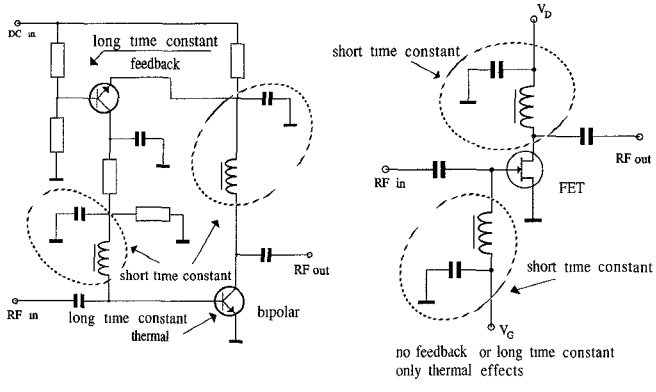

Fig. 12. Typical location of memory effects in the biasing circuit of bipolar and FET amplifiers.

"more linearly" for higher modulation frequencies. Taking into account the pulse distortion due to the bandwidth limitations of the NWA, the system described in this section is presently being modified to perform power swept measurements.

V. Typical Location of Memory Effects

The large-time-constant memory effects are typically due to the thermal time constants of the devices and to some of the components in the biasing circuit. Especially for bipolar devices, the structure of the biasing network (regulation of the base current as a function of the collector current) has an inherent time delay and causes long-time-constant memory effects. This effect is normally not present in FET amplifiers due to the more simplified biasing schemes and in particular to the absence of feedback loops.

The parasitics of the blocking coil and the resonance frequency of the blocking capacitor, as well as a proper grounding, are important parameters in reducing troublesome short-time memory effects.

Fig. 12 illustrates the most sensitive parts leading to memory effects in a widely used biasing circuit for bipolar amplifiers in comparison to FET amplifiers.

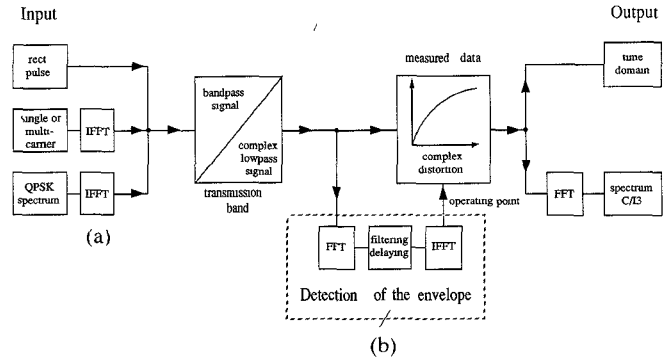

Fig. 13. Schematic of the extended computer model to simulate nonlinear systems with memory.

VI. Computer Simulation of Nonlinear Amplifiers

Starting with the measured single-carrier AM/AM and AM/PM characteristics of a nonlinear amplifier, together with the associated efficiency, the intermodulation products generated by a multicarrier input signal, the average efficiency, and the output power characteristic have been calculated for several amplifiers by means of a software package recently developed at ESTEC [8].

Since we are only interested in the intermodulation products falling within the transmission band of interest, the bandpass input signal is down-converted to a complex low-pass equivalent (2) and distorted by means of the measured and tabulated AM/AM and AM/PM data (see Fig. 13(a)).

Bandpass signal:

$$x_{BP}(t) = R(t) * \cos(\omega_c * t + \phi(t)).$$

Quadrature components:

$$v_i(t) = R(t) * \cos(\phi(t))$$
$$v_q(t) = R(t) * \sin(\phi(t)).$$

Complex low-pass equivalent:

$$x_{LP}(t) = 1/2 * R(t) * \exp(j * \phi(t)). \quad (2)$$

Performing an FFT, the distorted spectrum of the output signal and the C/I have been computed.

Referring to the first section of this paper, only quasi-memoryless systems can be analyzed and simulated with this computer model. In order to introduce memory effects, the model has been extended such that the envelope of the input signal is detected, filtered, delayed, and finally used as a controlling parameter to a set of different nonlinear transfer characteristics, previously measured for different operating points of the amplifier (Fig. 13(b)).

Now the nonlinear transfer characteristic (AM/AM and AM/PM conversion) is represented by a complex two-dimensional matrix with the input power and the operating point as input parameters and the output power and the phase as output parameters. For each sampling point of the input signal, the corresponding operating points and the amount of distortion can be calculated.

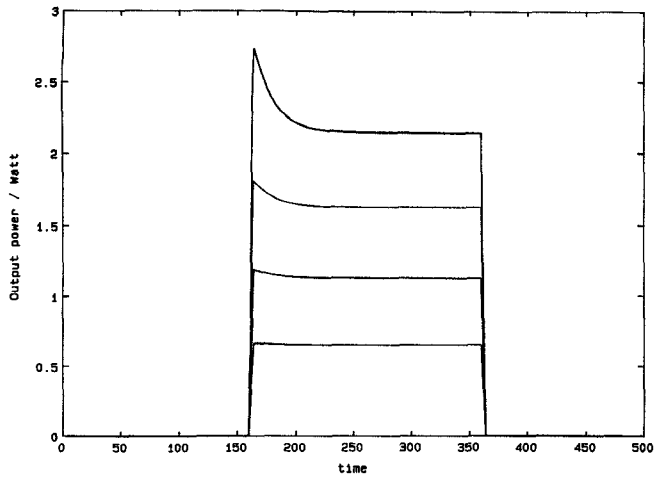

Fig. 14. Computed pulse response of a bipolar amplifier with memory.

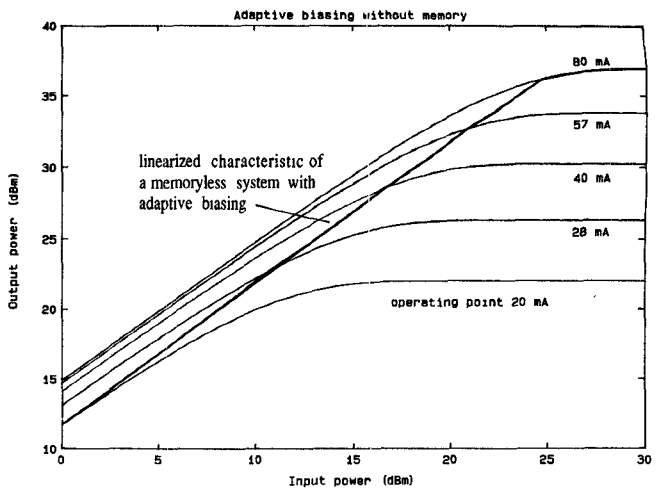

Fig. 15. Calculated P_{in}/P_{out} characteristics of an amplifier with adaptive biasing (ideal case), and the transfer characteristics at several operating points.

With this extended computer model, systems with memory can be simulated, and in particular, different biasing schemes and their memory effects can be analyzed. This capability can be applied, for example, to adaptive biasing amplifiers, where the biasing point of the active device is changed according to the input signal level. In general, the effects of feedback biasing circuits can also be predicted for different values of envelope frequencies.

Fig. 14, for example, shows the computed response of an amplifier using a constant current (feedback) biasing network for the bipolar power devices whose measured characteristics are reported in Fig. 11. Comparing the two figures, it is evident that good agreement is found over a wide dynamic range.

VII. Adaptive Linearization Techniques

By controlling the operating point of an amplifier according to the input signal envelope, the amplifier can be operated at constant gain, and thus the transfer characteristic can be linearized. In order to keep the characteristic linearized even under dynamic operation, the bandwidth of the controlling circuit should be far wider than the maximum modulation frequency.

Utilizing again the model of Fig. 13(b), the degradation in C/I due to the band limitations and time delays in the biasing network has been calculated. The amplifier's transfer characteristic at several operating points and the linearized characteristic in the ideal, memoryless case (no filtering and delaying) are illustrated in Fig. 15.

Introducing a time delay in the biasing circuit of only 10°, which corresponds to a 3 dB bandwidth of more than five times the maximum modulation frequency (in a simple RC section), the transfer characteristic shows a hysteresis (Fig. 16). For increasing input signal power the curve is undercompensated, and for decreasing values it is overcompensated (due to the time delay).

Fig. 17 shows the calculated third-order C/I with a two-carrier input signal as a function of different time delays in the biasing circuit. From this figure it appears that some improvement in C/I in the saturated region is

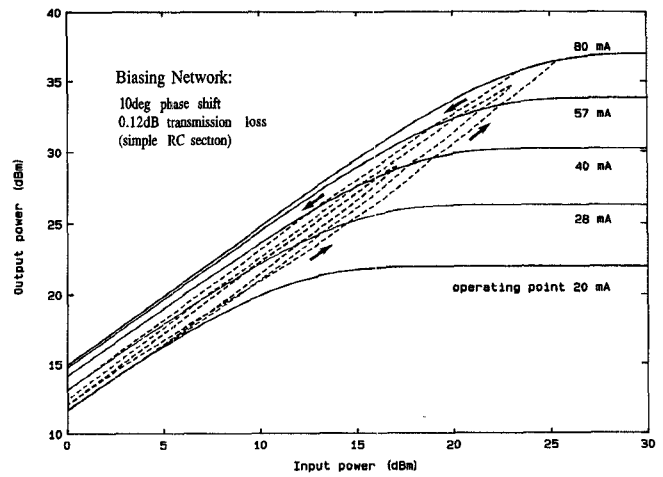

Fig. 16. Calculated P_{in}/P_{out} curve of an amplifier with memory in the adaptive biasing network.

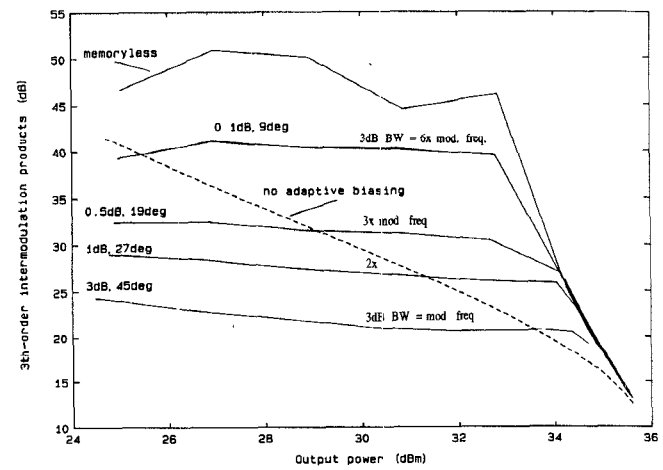

Fig. 17. Simulated degradation in $C/I3$ due to memory (time delay) in the adaptive biasing network.

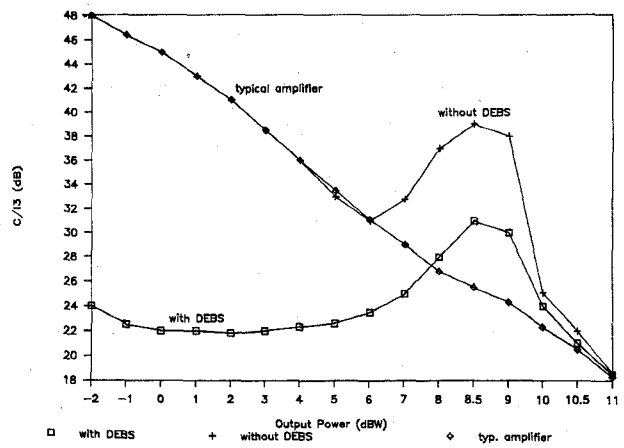

Fig. 18. Measured $C/I3$ of a power amplifier with and without adaptive biasing (DEBS).

achieved, but the linearity in the back-off region is reduced and the C/I degraded to about 25 dB.

These simulation results are in agreement with the intermodulation behavior in a practical adaptive biasing system (Dynamically Efficient Bias Scheme, DEBS, developed by Marconi Space Systems/Watford U.K., ESTEC contr. 5416/83/NL/GM), which is illustrated in Fig. 18. The improvement of the C/I in the saturated region without DEBS is due to cancellation effects inside the amplifier and not related to the memory of the system.

VIII. Conclusions

Detrimental effects of memories in linearizers have been described and two different, efficient techniques have been presented to measure them. These techniques allow a "real-time" adjustment and correction of the linearizer and/or amplifier circuits and an overall improvement of the intermodulation performance over a wide envelope frequency band.

This is especially important for broad-band applications, where high efficiency and linearity are required, and where memory effects, if not detected and properly corrected, may significantly degrade the system's performance.

Predistortion linearization in the presence of strong memory effects becomes extremely complex, if not impossible. In fact the compensation of the amplifier nonlinearities (amplitude and phase) is significantly affected and limited by the time delay characteristics of the system. A good knowledge of memory effects and of ways to detect and reduce them is also of extreme interest when alternative linearization methods are considered, such as adaptive biasing or loading techniques.

The simulation approach has proved to be useful in predicting the nonlinear response of practical systems with significant memory.

References

[1] A. M. Khilla, "Linearizers for power amplifiers in communication satellites," presented at the Workshop on Linearization Techniques, IEEE MTT-S Int. Microwave Symp., 1988.

[2] J. Czech, "A linearized L-band 200 Watt TWT amplifier for multicarrier operation," in *Proc. 16th European Microwave Conf.*, 1986, pp. 810–815.

[3] P. Hetrakul and D. P. Taylor, "Compensators for bandpass nonlinearities in satellite communications," *IEEE Trans. Aerosp. Electron. Syst.*, vol. AES-12, no. 4, pp. 509–514, July 1976.

[4] J. Minkoff, "Intermodulation noise in solid-state power amplifiers for wideband signal transmission," in *Proc. AIAA 9th Commun. Satellite Syst. Conf.*, 1982.

[5] O. Shimbo, "Effects of intermodulation, AM–PM conversion, and additive noise in multicarrier TWT systems," *Proc. IEEE*, vol. 59, pp. 230–238, Feb. 1971.

[6] M. Schetzen, *The Volterra and Wiener Theories of Nonlinear Systems*. New York: Wiley, 1980.

[7] W. Bösch, "Untersuchung zur Linearisierung und Leistungsoptimierung von bipolaren Leistungsverstärkern beim Vielträgerbetrieb im Satelliten-Mobilfunk," Ph.D dissertation, Tech. University of Graz, Austria, Nov. 1987.

[8] W. Bösch and G. Gatti, "IMAL software package to simulate the nonlinear systems response," ESTEC, Noordwijk, Netherlands, Nov. 1988.

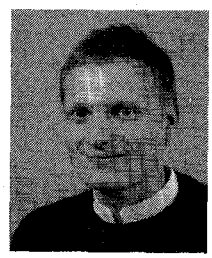

Wolfgang Bösch was born in Lustenau, Austria, on May 26, 1962. He received the Dipl.-Ing. degree in electrical engineering from the Technical University of Vienna, Austria, in 1985 and the Ph.D. degree in telecommunications from the Technical University of Graz, Austria, in 1988. His doctoral thesis dealt with various linearization techniques for power amplifiers in multicarrier operation.

In 1987 he joined the European Space Research and Technology Center (ESTEC) of the European Space Agency in Noordwijk, The Netherlands, where he is presently working as a research fellow in the RF-Systems Division in the field of advanced satellite communication systems. In particular he is engaged in nonlinear system simulation and the realization of high-efficiency power amplifiers. His research interests include solid-state power amplifiers, linearization techniques and their realization in advanced technologies (MMIC), and the simulation and measurement of nonlinear systems.

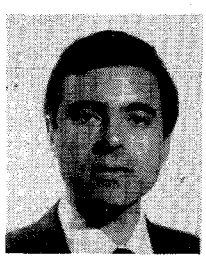

Giuliano Gatti (M'87) was born in Milan, Italy, in June 1954. He received the Dottore in Ingegneria Elettronica from the Politecnico di Milano in 1979.

Until 1984 he was with GTE-Telecomunicazioni in Milan, developing various MW hardware for satellite applications. From 1984 to 1986 he was project leader for a 4 GHz SSPA at SPAR-Aerospace in Montreal, Canada, where he was mainly involved in the development of MW amplifiers and isolators. Since 1986 he has been a Technical Specialist and Senior Engineer in the RF-Systems Department of the European Space Research and Technology Center (ESTEC) of the European Space Agency in Noordwijk, The Netherlands. He is engaged in various activities in the area of MW components and circuits for satellite hardware. His major research interests are solid-state power amplifiers, LNA's, up- and down-converters, linearizers, T/R modules, and beam-forming networks, as well as MIC and MMIC technologies.